Large Spin-Wave Energy Gap in the Bilayer Iridate Sr_{3}Ir_{2}O_{7}: Evidence for Enhanced Dipolar Interactions Near the Mott Metal-Insulator Transition

Jungho Kim, A. H. Said, D. Casa, M. H. Upton, T. Gog, M. Daghofer, G. Jackeli, J. van den Brink, G. Khaliullin, and B. J. Kim

Phys. Rev. Lett. **109**, 157402 — Published 10 October 2012

DOI: 10.1103/PhysRevLett.109.157402

Large Spin-Wave Energy Gap for the Bilayer Iridate $Sr_3Ir_2O_7$: Evidence for Enhanced Dipole-like Interactions near the Mott Metal-Insulator Transition

Jungho Kim,[1] A. H. Said,[1] D. Casa,[1] M. H. Upton,[1] T. Gog,[1] M. Daghofer,[2]
G. Jackeli,[3] J. van den Brink,[2] G. Khaliullin,[3] B. J. Kim[4]
[1]*Advanced Photon Source, Argonne National Laboratory, Argonne, Illinois 60439, USA*
[2]*Institute for Theoretical Solid Sate Physics, IFW Dresden, Helmholtzstr. 20, 01069 Dresden, Germany*
[3]*Max Planck Institute for Solid State Research, Heisenbergstraße 1, D-70569 Stuttgart, Germany and*
[4]*Materials Science Division, Argonne National Laboratory, Argonne, IL 60439, USA*
(Dated: August 27, 2012)

Using resonant inelastic x-ray scattering, we observe in the bilayer iridate $Sr_3Ir_2O_7$, a spin-orbit coupling driven magnetic insulator with a small charge gap, a magnon gap of ≈92 meV for both acoustic and optical branches. This exceptionally large magnon gap exceeds the total magnon bandwidth of ≈70 meV and implies a marked departure from the Heisenberg model, in stark contrast to the case of the single-layer iridate Sr_2IrO_4. Analyzing the origin of these observations, we find that the giant magnon gap results from bond-directional pseudo-dipolar interactions that are strongly enhanced near the metal-insulator transition boundary. This suggests that novel magnetism, such as that inspired by the Kitaev model built on the pseudo-dipolar interactions, may emerge in small charge-gap iridates.

PACS numbers: 74.10.+v, 75.30.Ds, 78.70.Ck

Identifying the hierarchy of energy scales associated with multiple interacting degrees of freedom is the starting point for understanding the physical properties of transition-metal oxides (TMOs). In most TMOs, the largest energy scale is the Coulomb interaction U, which suppresses charge motion in Mott insulators and allows description of the low-energy physics in terms of the remaining spin and orbital degrees of freedom. In $5d$ iridium oxides, however, U is significantly diminished due to the spatially extended $5d$ orbitals, and the correlated insulating state cannot be sustained without the aid of large spin-orbit coupling (∼0.5 eV) [1]. This additional interaction competes with other energy scales such as the crystal field and the hopping amplitude. The resulting charge gap is much smaller than that in a typical $3d$ TMO or even those in most semiconductors, being on the order of 0.1 eV or even smaller [2, 3]. On the other hand, the energy scale of the magnetic interaction has been recently found to be of the same order of magnitude as that of $3d$ TMOs [4, 5]. As a consequence, an intriguing new hierarchy may result in which the energy scales for magnetic degrees of freedom surpass that for charge degrees of freedom, ushering in a new paradigm for the magnetism in $5d$ TMOs.

Iridates of the Ruddlesden-Popper series $Sr_{n+1}Ir_nO_{3n+1}$ display a systematic electronic evolution as a function of the number of IrO_2 layers (n): as n increases, the electronic structure progresses toward a metallic ground state as evidenced by the softening of the charge gap in $Sr_3Ir_2O_7$ (n=2) and the metallic state found for $SrIrO_3$ (n=∞) [3]. The charge gap becomes so small already at n=2 that it cannot be resolved even in the optical conductivity spectrum, indicating proximity to the Mott transition point. Thus, the bilayer compound $Sr_3Ir_2O_7$ provides a platform for investigating the nature of magnetism near the metal-insulator transition (MIT) boundary.

In this Letter, we report the magnetic excitation spectra of $Sr_3Ir_2O_7$ measured by resonant inelastic x-ray scattering (RIXS) [6], which show a number of features characterizing the unconventional nature of the magnetism in $Sr_3Ir_2O_7$ lying close to a Mott critical point. We observe two anomalous features: a giant magnon gap of ≈92 meV, even larger than the total magnon bandwidth ≈70 meV, which demonstrates a marked departure from the Heisenberg model; and a very small bilayer splitting (≈5 meV), which is surprising in view of the "cubic" shape of the spin-orbit entangled wavefunction in iridates [7, 8], which would suggest strong inter-layer interactions. The observed small bilayer splitting indicates frustration of the inter-layer isotropic exchange interactions. The temperature scale of the magnon gap exceeds 1000 K, indicating that the melting of the G-type collinear antiferromagnetic (AF) order [9, 10] at ≈285 K is not driven by thermal fluctuations of magnetic moments, but rather by thermal charge carriers. Our analysis shows that the large magnon gap results from enhanced pseudo-dipolar (PD) interactions, which has an intriguing implication for the Kitaev model [11] discussed recently in the context of honeycomb lattice iridates A_2IrO_3 (A=Li or Na) in which the PD interactions play the major role [8, 12–17].

Experiments were carried out at the 30-ID beamline at the Advanced Photon Source. A horizontal scattering geometry was used with π-polarized incident photons tuned to Ir L_3 edge. A spherical diced Si(844) analyzer was used. The overall energy and momentum resolution of the RIXS spectrometer was about 30 meV and ±0.032 $\AA^{-1}$, respectively. By using a high resolution monochro-

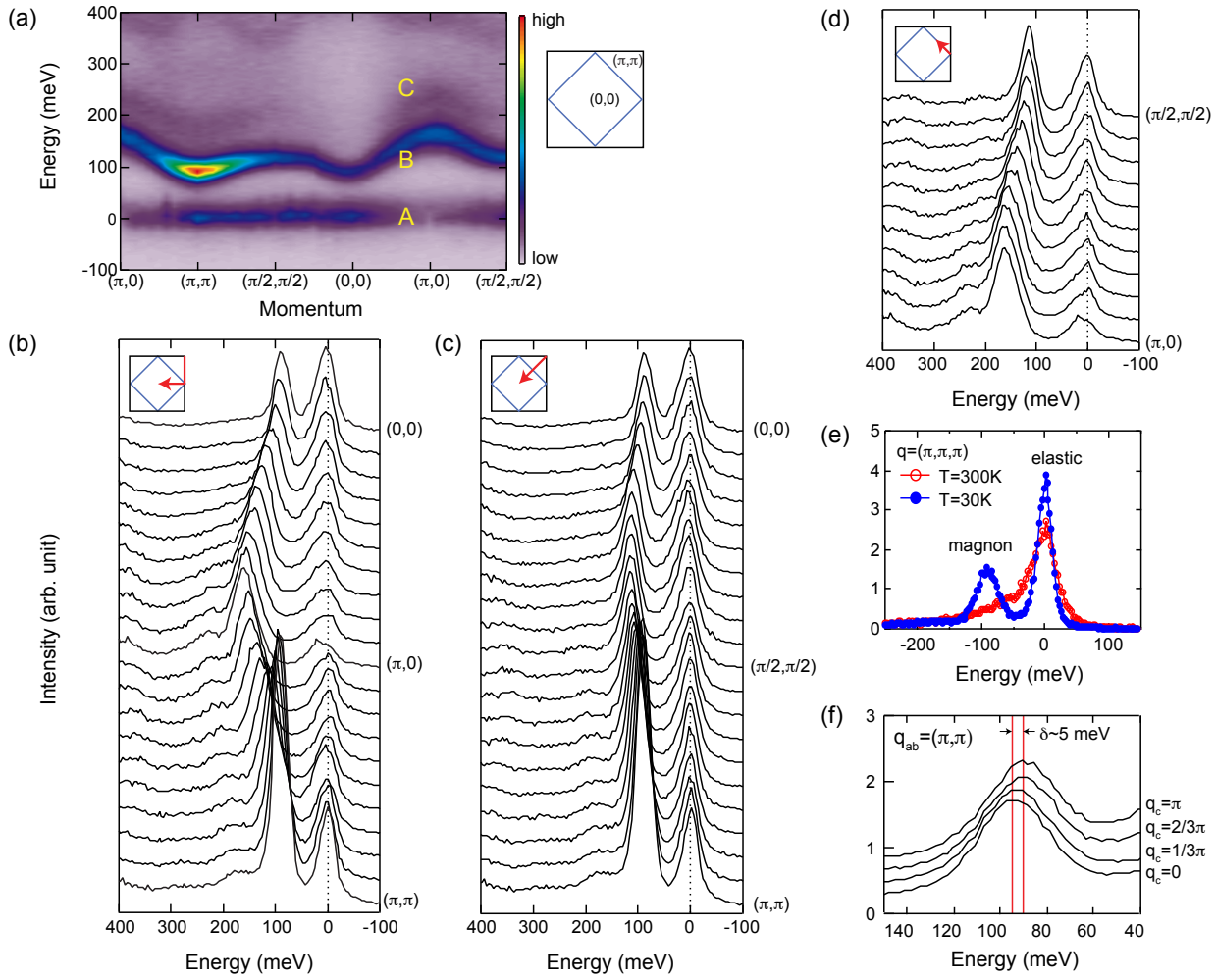

FIG. 1. (a) Image and (b-d) stack plot of the RIXS data recorded at T= 30 K with q_{ab} along high symmetry lines and q_c fixed at $\frac{\pi}{3}$. Brillouin zone of the undistorted tetragonal unit cell (black square) and the magnetic cell (blue square) is shown with the notation following the convention for the tetragonal unit cell, as, for instance, in La_2CuO_4. (e) RIXS spectra measured at the ordering vector $\mathbf{q}=(\pi,\pi,\pi)$ above (red open circle) and below (blue solid circle) $T_N \approx 285$ K. (f) RIXS spectra at four different q_c's with q_{ab} fixed at (π,π). The q_c's of 0, $\pi/3$, $2\pi/3$, and π correspond approximately to l=25.65, 26.5, 27.35, and 28.25, respectively. Spectra are vertically offset for clarity. The red lines mark the approximate peak positions at q_c=0 and π.

mator and improving the quality of the analyzer, the energy resolution has been improved by more than a factor of four since we recently reported RIXS measurement on the single layer iridate Sr_2IrO_4 [4].

Figures 1(a) and 1(b)-(d) show the image and stack plots, respectively, of the RIXS spectra recorded with in-plane momentum transfer q_{ab} along high symmetry lines and q_c fixed at $\frac{\pi}{3}$. Three main features in the spectra are: (A) elastic/quasi-elastic peaks near the zero energy, (B) an intense and dispersive band in the range 90∼160 meV, and (C) a rather weak and broad feature above the dipersive band suggestive of two-magnon states. We assign the feature (B) to a single magnon excitation based on the fact that it is highly sensitive to the magnetic transition [see Fig. 1(e)] and that its intensity is peaked at the magnetic ordering vector (π,π) (see also Fig. 2). In the single layer Sr_2IrO_4, it has been seen in a RIXS experiment that the single magnon excitation lie in the similar energy window [4].

With this assignment, however, two anomalies are apparent: the acoustic branch appears to be absent, and the magnon gap is unusually large even for an optical mode. Typically, two branches of magnetic modes, acoustic and optical, are observed in other bilayer systems such as bilayer manganites [18] and cuprates [19]. To identify the acoustic branch, we scanned along the q_c direction fixing $q_{ab}=(\pi,\pi)$ where the maximal bilayer splitting is expected, as shown in Fig. 1(f). At $q_c=\pi$ (0), only the acoustic (optical) branch has finite intensity, in accordance with the intuitive notion that magnons emanate from magnetic Bragg spots. At intermediate q_c, the spectrum is contributed to by both branches with a gradual shift in spectral weight from one branch to the other. We see an upward shift of ≈5 meV as q_c is varied from π to 0.

Thus, it is seen that the acoustic branch also has a large gap and is nearly degenerate with the optical branch. The small splitting of the two branches implies strongly frustrated inter-layer interactions, which, at first sight, seems inconsistent with the observed spin-flop transition driven by the inter-layer interactions [9].

To unravel this paradox, we first determine the origin of the anomalously large magnon gap. Such a large gap signals a marked departure from the Heisenberg model and that the magnetism in bilayer $Sr_3Ir_2O_7$ is therefore qualitatively different from its single layer variant Sr_2IrO_4. A recent resonant x-ray diffraction study [9] establishes that $Sr_3Ir_2O_7$ has a c-axis collinear structure, unlike the single layer Sr_2IrO_4 with in-plane canted moments [7]. These different magnetic anisotropies in Sr_2IrO_4 and $Sr_3Ir_2O_7$ were captured in a magnetic exchange Hamiltonian derived from microscopic interactions, which we will use here as well, adding to it longer-range interaction terms, which were also needed in the single layer Sr_2IrO_4 to quantitatively account for the magnon dispersion [4]. The model contains intra- and inter-layer interactions; the intra-layer interactions read

$$H_{ab} = \sum_{\langle i,j\rangle}\Big[J\vec{S}_i\vec{S}_j + \Gamma S_i^z S_j^z + D\big(S_i^x S_j^y - S_i^y S_j^x\big)\Big] + \sum_{\langle\langle i,j\rangle\rangle} J_2\vec{S}_i\vec{S}_j + \sum_{\langle\langle\langle i,j\rangle\rangle\rangle} J_3\vec{S}_i\vec{S}_j\ , \quad (1)$$

where $\langle i,j\rangle$, $\langle\langle i,j\rangle\rangle$, and $\langle\langle\langle i,j\rangle\rangle\rangle$ denote first, second and third nearest neighbors within each plane, and J, J_2 and J_3 represent the corresponding isotropic coupling constants [see Fig. 3(a)]. The anisotropic coupling Γ includes PD terms driven by Hund's exchange and those due to staggered rotations of octahedra [8]. The latter also induce a Dzyaloshinsky-Moriya (DM) interaction, with the corresponding coupling constant D. Analogously, the inter-layer interactions read

$$H_c = \sum_i\Big[J_c\vec{S}_i\vec{S}_{i+z} + \Gamma_c S_i^z S_{i+z}^z + D_c\big(S_i^x S_{i+z}^y - S_i^y S_{i+z}^x\big)\Big] + \sum_{\langle i,j\rangle} J_{2c}\vec{S}_i\vec{S}_{j+z}\ , \quad (2)$$

where the first sum runs over all sites in one plane, and the second over all next-nearest-neighbor pairs across the planes [see Fig. 3(a)]. Inter-layer interactions J_c, Γ_c, and D_c for nearest-neighbors along c are complemented by an inter-layer next-nearest–neighbor coupling J_{2c}.

In this model, the magnon dispersions are given by

$$\omega_\pm(\mathbf{q}) = S\sqrt{A_\pm^2(\mathbf{q}) - X_\pm^2(\mathbf{q}) - Y_\pm^2(\mathbf{q})} \quad (3)$$

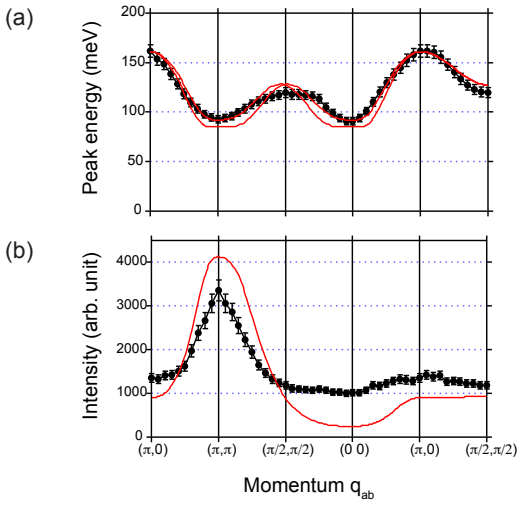

FIG. 2. Momentum dependence of the (a) position and (b) intensity of the magnon peak extracted by fitting the RIXS spectra (dots with error bar), overlaid with the fit from theory model at θ=0.26π and η=0.24 (red solid lines). Because the acoustic and optical branches are not resolved in the experiment, the intensities for the two branches are summed in the theoretical calculations with appropriate weights (see *Supplementary Material* for details) to compare to the experiment.

with

$$A_\pm(\mathbf{q}) = 4(J+\Gamma) + (J_c+\Gamma_c) - 4J_2(1-\cos q_x\cos q_y) - 4J_3(1-\gamma_{2\mathbf{q}}) - 4J_{2c}(1\mp\gamma_{\mathbf{q}})\ , \quad (4)$$

$$X_\pm(\mathbf{q}) = 4J\gamma_{\mathbf{q}} \pm J_c,\ Y_\pm(\mathbf{q}) = 4D\gamma_{\mathbf{q}} \pm D_c\ , \quad (5)$$

where the upper (lower) sign refers to optical (acoustic) branches, and $\gamma_{\mathbf{q}} = \frac{1}{2}(\cos q_x + \cos q_y)$.

Following Ref. [8], one can express all the isotropic and anisotropic exchange coupling constants (except the ones for the long-range interactions J_2,J_3 and J_{2c}), in terms of the two microscopic parameters η and θ, and thus fit the magnon spectrum using these parameters. Here, η=J_H/U is the ratio between Hund's coupling and Coulomb correlation, and θ parametrizes the degree of tetragonal distortion. Note that the PD interactions in the strong SOC limit are scaled by η [8], and θ describing the deviation from the cubic wavefunction ($J_{\rm eff}$=1/2) is directly relevant to hopping amplitudes and therefore the superexchange interactions. The expressions for the dependences of the coupling constants on these parameters are provided in the *Supplemental Material*. This approach greatly reduces the number of adjustable parameters; in particular, the magnon gap is controlled only by the two parameters η and θ.

Figure 2 shows the fit of the experimental dispersion and intensity using the above model. We find that the large gap can only be reproduced when both θ and η are large: θ=$(0.26\pm0.01)\pi$ and η=0.23$\sim$0.27. Thus, the observed large gap alone almost uniquely fixes all nearest-neighbor couplings expressed in terms of η and θ [20].

TABLE I. Coupling constants (in units of meV) determined from fits to the experimental magnon dispersion through the microscopic model in Refs. [8, 9] at the representative values of θ=0.26π and η=0.24. *Supplemental Material* provides details on the stability of the fit.

J	J_c	J_2	J_3	J_{2c}	Γ	Γ_c	D	D_c
93	25.2	11.9	14.6	6.2	4.4	34.3	24.5	28.1

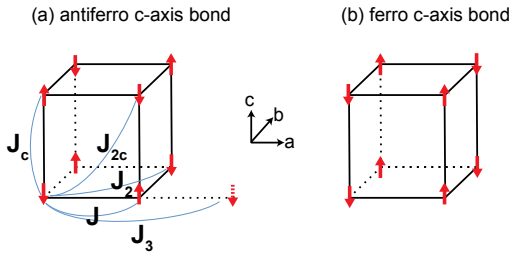

FIG. 3. (a) Ground state magnetic structure of $Sr_3Ir_2O_7$. (b) A magnetic state with nearly the same energy when only Heisenberg couplings are considered.

Physically, large η can be understood as arising from the screening of U as the system approaches the borderline of an MIT, which is evident from the optical data showing softening of the charge gap [2]. It is well known that while U is screened in the solid, J_H is not [21, 22], so that the metallic screening results in enhanced η. The need for the large θ can be seen from the fact that when θ is larger than $\theta_c(\approx 0.25\pi)$, both in-plane ($\Gamma$) and out-of-plane ($\Gamma_c$) PD terms favor the c-axis moment [9] and thus there is a strong preference for the c-axis moment. This pronounced magnetic anisotropy is amplified by the large η, which leads to the sizable gap. While DM terms also contribute to the stabilization of the c-easy axis structure [9], their effects in the magnon dispersion are much smaller than those from the PD terms. The long-range interactions, J_2,J_3 and J_{2c}, serve to fine tune the shape of the dispersion [20], but they are irrelevant to our main finding that the enhanced PD coupling results in the large magnon gap. With this we find the exchange parameters shown in Table 1. In addition to very large anisotropic couplings, we find that the nearest-neighbor Heisenberg coupling J is also enhanced compared to its measured [4] and theoretically estimated [23, 24] values in Sr_2IrO_4.

We now return to the discussion of the small bilayer splitting. Among the long-range interaction terms that were included (J_2, J_3, and J_{2c}), J_{2c} plays a critical role in determining the bilayer splitting. In a pure Heisenberg model, a small bilayer splitting would imply a small energy difference between the two magnetic configurations shown in Fig. 3, and the coupling constants in Tab. 1 corroborate this with $J_c \approx 4J_{2c}$ (J_{2c} couples to four sites and thus cancels a four times stronger J_c). However, Eqs. (4) and (5) show that the PD interactions do not contribute to the bilayer splitting but considerably lower the energy of the G-type AF order in Fig. 3(a).

The interesting situation arises that even if the inter-layer *isotropic* exchange interactions are almost completely frustrated, the layers are still strongly coupled by the inter-layer PD and DM interactions that are responsible for the magnetic anisotropy. The strong inter-layer PD interactions manifested by the large gap do not conflict with the small bilayer splitting since PD terms, having the Ising form, do not propagate magnons between the planes.

The observed large magnon gap has two important implications. First, it raises the question as to how the magnetic order melts at a temperature scale ($T_N \approx 285$ K) much smaller than the magnon gap ($\Delta_m > 1000$ K). The rapid drop in the electrical resistivity when the system is heated through T_N [25] suggests that the transport properties are correlated with the magnetic order. However, the observed large magnon gap can hardly be reconciled with the standard single band spin-density wave picture with isotropic spin dynamics. Given that the charge gap (even unresolved in the optical data) might be very small, it is likely that AF order is destroyed by thermally activated charge carriers that form magnetic polarons, whose motion is known to be particulary detrimental for an Ising-type magnetic order with large magnon gap that prevents a coherent charge propagation [26]. Whether this thermal-carrier-driven magnetic transition is a special case for $Sr_3Ir_2O_7$ or can be generally applied to other $5d$ TMOs with small charge gap [27, 28] remains to be explored both experimentally and theoretically.

Second, the enhanced PD interactions suggest a direction for realization of the Kitaev model discussed in related iridates A_2IrO_3 (A=Li or Na). In an ideal geometry where Ir ions sit on the vertices of a honeycomb lattice and are connected by edge-sharing oxygen octahedra, it has been shown that the isotropic exchange interactions are strongly reduced for the cubic $J_{\rm eff}$=1/2 wavefunction and the PD terms render a realization of the Kitaev model with a spin liquid ground state [8, 12]. Experimentally, however, both Li_2IrO_3 and Na_2IrO_3 are known to have long-range order at $T_N \approx 15$ K [13–15], which signals strong perturbation by the Heisenberg term. This is possibly due to less-than-ideal realization of the Kitaev model in these compounds. Our study shows that approaching the MIT boundary in favor of large J_H/U may enhance the PD term and stabilize the spin-liquid ground state. In this regard, high pressure experiments on these iridates may be interesting.

To summarize, we have revealed the unconventional nature of the magnetism in a spin-orbit entangled Mott insulator $Sr_3Ir_2O_7$ lying on the verge of MIT. The system shows a marked departure from the Heisenberg model due to the strongly enhanced PD interactions. In contrast to $3d$ oxides with small spin-orbit coupling that

can be described by isotropic Heisenberg interactions with small anisotropic corrections, $Sr_3Ir_2O_7$ exemplifies how a novel type of magnet can arise from a $5d$ oxide with strong spin-orbit coupling and a small charge gap. Our findings should have profound implications for other iridium compounds with lattice geometries in which the Heisenberg term is strongly suppressed.

Work in the Material Science Division and the use of the Advanced Photon Source at the Argonne National Laboratory was supported by the U.S. DOE under Contract No. DE-AC02-06CH11357. G.J. acknowledges support from GNSF/ST09-447. M.D. acknowledges support from the DFG (Emmy-Noether program).

[1] B. J. Kim, H. Jin, S. J. Moon, J.-Y. Kim, B.-G. Park, C. S. Leem, J. Yu, T. W. Noh, C. Kim, S.-J. Oh, J.-H. Park, V. Durairaj, G. Cao, and E. Rotenberg, Phys. Rev. Lett., **101**, 076402 (2008).

[2] S. J. Moon, H. Jin, W. S. Choi, J. S. Lee, S. S. A. Seo, J. Yu, G. Cao, T. W. Noh, and Y. S. Lee, Phys. Rev. B, **80**, 195110 (2009).

[3] S. J. Moon, H. Jin, K. W. Kim, W. S. Choi, Y. S. Lee, J. Yu, G. Cao, A. Sumi, H. Funakubo, C. Bernhard, and T. W. Noh, Phys. Rev. Lett., **101**, 226402 (2008).

[4] J. Kim, D. Casa, M. H. Upton, T. Gog, Y.-J. Kim, J. F. Mitchell, M. van Veenendaal, M. Daghofer, J. van den Brink, G. Khaliullin, and B. J. Kim, Phys. Rev. Lett., **108**, 177003 (2012).

[5] S. Fujiyama, H. Ohsumi, T. Komesu, J. Matsuno, B. J. Kim, M. Takata, T. Arima, and H. Takagi, Phys. Rev. Lett., **108**, 247212 (2012).

[6] For a review of RIXS method, see L. J. P. Ament, M. van Veenendaal, T. P. Devereaux, J. P. Hill, and J. van den Brink, Rev. Mod. Phys., **83**, 704 (2011).

[7] B. J. Kim, H. Ohsumi, T. Komesu, S. Sakai, T. Morita, H. Takagi, and T. Arima, Science, **323**, 1329 (2009).

[8] G. Jackeli and G. Khaliullin, Phys. Rev. Lett., **102**, 017205 (2009).

[9] J. W. Kim, Y. Choi, J. Kim, J. F. Mitchell, G. Jackeli, M. Daghofer, J. van den Brink, G. Khaliullin, and B. J. Kim, Phys. Rev. Lett., **109**, 037204 (2012).

[10] S. Boseggia, R. Springell, H. C. Walker, A. T. Boothroyd, D. Prabhakaran, D. Wermeille, L. Bouchenoire, S. P. Collins, and D. F. McMorrow, Phys. Rev. B, **85**, 184432 (2012).

[11] A. Kitaev, Ann. Phys. (N.Y.), **321**, 2 (2006).

[12] J. Chaloupka, G. Jackeli, and G. Khaliullin, Phys. Rev. Lett., **105**, 027204 (2010).

[13] Y. Singh and P. Gegenwart, Phys. Rev. B, **82**, 064412 (2010).

[14] X. Liu, T. Berlijn, W.-G. Yin, W. Ku, A. Tsvelik, Y.-J. Kim, H. Gretarsson, Y. Singh, P. Gegenwart, and J. P. Hill, Phys. Rev. B, **83**, 220403 (2011).

[15] Y. Singh, S. Manni, J. Reuther, T. Berlijn, R. Thomale, W. Ku, S. Trebst, and P. Gegenwart, Phys. Rev. Lett., **108**, 127203 (2012).

[16] S. K. Choi, R. Coldea, A. N. Kolmogorov, T. Lancaster, I. I. Mazin, S. J. Blundell, P. G. Radaelli, Y. Singh, P. Gegenwart, K. R. Choi, S.-W. Cheong, P. J. Baker, C. Stock, and J. Taylor, Phys. Rev. Lett., **108**, 127204 (2012).

[17] F. Ye, S. Chi, H. Cao, B. C. Chakoumakos, J. A. Fernandez-Baca, R. Custelcean, T. Qi, O. B. Korneta, and G. Cao, Phys. Rev. B, **85**, 180403 (2012).

[18] T. G. Perring, D. T. Adroja, G. Chaboussant, G. Appeli, T. Kimura, and Y. Tokura, Phys. Rev. Lett., **87**, 217201 (2001).

[19] D. Reznik, P. Bourges, H. F. Fong, L. P. Regnault, J. Bossy, C. Vettier, D. L. Milius, I. A. Aksay, and B. Keimer, Phys. Rev. B, **53**, 14741 (1996).

[20] See *Supplemental Material* for theory details.

[21] E. Antonides, E. C. Janse, and G. A. Sawatzky, Phys. Rev. B, **15**, 1669 (1979).

[22] A. Bosch, H. Feil, G. A. Sawatzky, and N. Martensson, Solid State Commun., **34**, 141 (1980).

[23] V. Katukuri, H. Stoll, J. van den Brink, and L. Hozoi, Phys. Rev. B, **85**, 220402(R) (2012).

[24] B. H. Kim, G. Khaliullin, and B. I. Min, arXiv:1205.3289.

[25] G. Cao, Y. Xin, C. S. Alexander, J. E. Crow, P. Schlottmann, M. K. Crawford, R. L. Harlow, and W. Marshall, Phys. Rev. B, **66**, 214412 (2002).

[26] C. L. Kane, P. A. Lee, and N. Read, Phys. Rev. B, **39**, 6880 (1989).

[27] S. Calder, V. O. Garlea, D. F. McMorrow, M. D. Lumsden, M. B. Stone, J. C. Lang, J.-W. Kim, J. A. Schlueter, Y. G. Shi, K. Yamaura, Y. S. Sun, Y. Tsujimoto, and A. D. Christianson, Phys. Rev. Lett., **108**, 257209 (2012).

[28] D. Hsieh, F. Mahmood, D. H. Torchinsky, G. Cao, and N. Gedik, Phys. Rev. B, **86**, 035128 (2012).